S-wave contributions to $\bar{B}_s^0 \to (D^0, \bar{D}^0)\pi^+\pi^-$ in the perturbative QCD framework*

Ye Xing(邢晔)[1)] Zhi-Peng Xing(邢志鹏)[2)]

INPAC, SKLPPC, MOE Key Laboratory for Particle Physics, School of Physics and Astronomy, Shanghai Jiao Tong University, Shanghai 200240, China

Abstract: $\bar{B}_s^0 \to (D^0, \bar{D}^0)\pi^+\pi^-$ is induced by the $b \to c\bar{u}s/b \to u\bar{c}s$ transitions, which can interfere if a CP-eigenstate $D_{\rm CP}$ is formed. The interference contribution is sensitive to the CKM angle γ. In this work, we study the *S*-wave $\pi^+\pi^-$ contributions to the process in the perturbative QCD factorization. In the factorization framework, we adopt two-meson light-cone distribution amplitudes, whose normalization is parametrized by the *S*-wave time-like two-pion form factor with resonance contributions from $f_0(500)$, $f_0(980), f_0(1500), f_0(1790)$. We find that the branching ratio of $\bar{B}_s^0 \to (D^0, \bar{D}^0)(\pi^+\pi^-)_S$ is of the order of 10^{-6}, and that significant interference exists in $\bar{B}_s^0 \to D_{\rm CP}(\pi^+\pi^-)_S$. Future measurement could not only provide useful constraints on the CKM angle γ, but would also be helpful for exploring the multi-body decay mechanism of heavy mesons.

Keywords: PQCD, three bodys decays, γ angle

PACS: 12.38-t **DOI:** 10.1088/1674-1137/43/7/073103

1 Introduction

In recent years, three-body hadronic B/B_s meson decays have attracted considerable attention of the experiments [1-3]. These processes provide new ways of studying the phenomenology of the Standard Model and of probing new physics effects. For instance, the LHCb collaboration has measured sizable direct CP asymmetries in the phase space of the three-body B decays [4, 5]. In addition, these processes are also valuable for understanding the mechanism of multi-body heavy meson decays.

On the theoretical side, the perturbative QCD (PQCD) framework, based on the k_T factorization, has been applied to analyze the B/B_s semi-leptonic and two-body decays processes [6-30]. The PQCD framework has also been used to study three-body decays [31-41]. Generally, the multi-scale decay amplitude may be written as a convolution, including the nonperturbative wave functions, hard kernel at the intermediate scale and short-distance Wilson coefficients. The factorization is greatly simplified if two of the final hadrons move collinearly. In this case, the three-body decays are reduced to quasi-two-body processes. Therefore, nonperturbative wave functions include two-meson light-cone distributions, which contain both resonant and nonresoant contributions. For instance, the measurement of $B_s \to J/\psi(\pi^+\pi^-)_S$ by LHCb [5] indicates that the resonances $f_0(500)$, $f_0(980)$, $f_0(1500)$, $f_0(1790)$ of the *S*-wave $\pi\pi$-pair are dominant, which is confirmed by the theoretical calculation in the framework of PQCD [42-47]. In this work, we focus on $\bar{B}_s^0 \to D^0(\bar{D}^0)\pi^+\pi^-$ and include the $B_s \to D(f_0(500)+f_0(980)+f_0(1500)+f_0(1790)) \to D[(\pi^+\pi^-)_S]$ contributions. More explicitly, a Breit-Wigner (BW) model is used for the resonances $f_0(500), f_0(1500)$, $f_0(1790)$ [48] , and the Flatté model is adopted for the resonance $f_0(980)$ [49]. $\bar{B}_s^0 \to D^0(\bar{D}^0)\pi^+\pi^-$, with the CP eigenstate containing the interference amplitude from $b \to c\bar{u}s$ ($b \to u\bar{c}s$), is sensitive to the angle γ of the CKM Unitarity Triangle, whose precise measurement is one of the primary objectives in flavour physics.

The paper is organized as follow: in Sec. 2, we introduce the wave functions of B_s, D and of the two pions. Sec. 3 contains our perturbative calculation within the

Received 12 March 2019, Published online 10 June 2019

* Supported in part by National Natural Science Foundation of China (11575110, 11735010), Natural Science Foundation of Shanghai (15DZ2272100), Key Laboratory for Particle Physics, Astrophysics and Cosmology, Ministry of Education

1) E-mail: xingye_guang@sjtu.edu.cn

2) E-mail: zpxing@sjtu.edu.cn

PQCD framework. In Sec. 4, we give the numerical results, and a conclusion is presented in the last section.

2 Wave functions

In general, the wave function $\Phi_{\alpha\beta}$ with Dirac indices α,β can be decomposed into 16 independent components, $I_{\alpha\beta},\gamma^{\mu}_{\alpha\beta},(\gamma^{\mu}\gamma^{5})_{\alpha\beta},\gamma^{5}_{\alpha\beta},\sigma^{\mu\nu}_{\alpha\beta}$. For the pseudoscalar B_s meson, the light-cone matrix element is defined as

$$\int_0^1 \frac{d^4z}{(2\pi)^4} e^{ik_1\cdot z}\langle 0|b_\alpha(0)\bar{q}_\beta(z)|\bar{B}_s(P_{B_s})\rangle = \frac{i}{\sqrt{2N_c}}\left\{(\not P_{B_s}+m_{B_s})\gamma_5\left[\phi_{B_s}(k_1)+\frac{\not n-\not v}{\sqrt{2}}\bar{\phi}_{B_s}(k_1)\right]\right\}_{\alpha\beta}, \quad (1)$$

where the light-cone vectors are $\boldsymbol{n}=(1,0,0_T)$ and $\boldsymbol{v}=(0,1,0_T)$. The two independent parts of the B_s meson light-cone distribution amplitude obey the following normalization conditions:

$$\int \frac{d^4k_1}{(2\pi)^4}\phi_{B_s}(k_1)=\frac{f_{B_s}}{2\sqrt{2N_c}}, \quad \int \frac{d^4k_1}{(2\pi)^4}\bar{\phi}_{B_s}(k_1)=0, \quad (2)$$

where f_{B_s} is the decay constant of B_s meson. Since the contribution of $\bar{\phi}_{B_s}(k_1)$ is numerically small [28], we neglect it and keep only the $\phi_{B_s}(k_1)$ part in the above equation. In the momentum space the light-cone matrix of B_s meson can be expressed as follows:

$$\Phi_{B_s}=\frac{i}{\sqrt{2N_c}}(\not P_{B_s}+m_{B_s})\gamma_5\phi_{B_s}(k_1). \quad (3)$$

Usually, the hard part is independent of k^+ or/and k^-, thus one can integrate one of them out from $\phi_{B_s}(k^+,k^-,k_\perp)$. With b as the conjugate space coordinate of $k_\perp$, we can express $\phi_{B_s}(x,k_\perp)$ in the b-space by

$$\Phi_{B_s}(x,b)_{\alpha\beta}=\frac{i}{\sqrt{2N_c}}[(\not P_{B_s}+m_{B_s})\gamma_5]_{\alpha\beta}\phi_{B_s}(x,b), \quad (4)$$

where x is the momentum fraction of the light quark in B_s meson. In this paper, we adopt the following expression for $\phi_{B_s}(x,b)$

$$\phi_{B_s}(x,b)=N_{B_s}x^2(1-x)^2\exp\left[-\frac{m_{B_s}^2x^2}{2\omega_b^2}-\frac{(\omega_b b)^2}{2}\right], \quad (5)$$

where N_{B_s} is the normalization factor, which is determined by the above equation with $b=0$. In our calculation, we adopt $\omega_b=(0.50\pm0.05)$GeV [9] and $f_{B_s}=(0.228\pm 0.004)$GeV [10], from which we determine $N_{B_s}=63.02$.

The wave function of the charmed D meson, treated as the heavy-light system, is defined by the light-cone matrix element as follows [11]:

$$\int_0^1 \frac{d^4z}{(2\pi)^4}e^{ik_2\cdot z}\langle 0|\bar{c}_\alpha(0)q_\beta(z)|\bar{D}^0(P_D)\rangle = -\frac{i}{\sqrt{2N_c}}\left\{(\not P_D+m_D^0)\gamma_5\phi_D(k_2)\right\}_{\beta\alpha}, \quad (6)$$

which satisfies the normalization

$$\int \frac{d^4k_2}{(2\pi)^4}\phi_D(k_2)=\frac{f_D}{2\sqrt{2N_c}}. \quad (7)$$

Here, f_D is the decay constant, and the chiral D meson mass is taken as $m_D^0=\frac{m_D^2}{m_c+m_d}=m_D+O(\Lambda)$. For the numerical calculation, we adopt the parametrization [50],

$$\phi_D(x_2,b_2)=\frac{f_D}{2\sqrt{2N_c}}6x_2(1-x_2)[1+C_D(1-2x_2)] \times\exp\left[-\frac{\omega_D^2b_2^2}{2}\right], \quad (8)$$

where the free shape parameter C_D is $C_D=0.5\pm0.1$ [14], and f_D, ω_D read as $f_D=0.209\pm0.002$ [10] and $\omega_D=0.1$ [14].

The S-wave two-pion distribution amplitude is then given as [46]

$$\Phi_{\pi\pi}^{S-\mathrm{wave}}=\frac{1}{\sqrt{2N_c}}[\not p\Phi_{\pi\pi}(z,\xi,m_{\pi\pi}^2)+m_{\pi\pi}\Phi_{\pi\pi}^s(z,\xi,m_{\pi\pi}^2) +m_{\pi\pi}(\not n\not v-1)\Phi_{\pi\pi}^T(z,\xi,m_{\pi\pi}^2)], \quad (9)$$

where z is the momentum fraction carried by the spectator positive quark, $\Phi_{\pi\pi}$, $\Phi_{\pi\pi}^s$ and $\Phi_{\pi\pi}^T$ are twist-2 and twist-3 distribution amplitudes. $m_{\pi\pi}$ is the invariant mass of the pion pair. We consider that the two-pion system moves in the n direction. ξ as the momentum fraction of π^+ in the pion pair. The asymptotic forms are parametrized as [51-53]

$$\Phi_{\pi\pi}=\frac{F_s(m_{\pi\pi}^2)}{2\sqrt{2N_c}}a_2 6z(1-z)3(2z-1),$$
$$\Phi_{\pi\pi}^s=\frac{F_s(m_{\pi\pi}^2)}{2\sqrt{2N_c}},\ \Phi_{\pi\pi}^T=\frac{F_s(m_{\pi\pi}^2)}{2\sqrt{2N_c}}(1-2z). \quad (10)$$

Here, $F_s(m_{\pi\pi}^2)$ and a_2 are the timelike scalar form factor and the Gegenbauer coefficient, respectively. As a first approximation, the S-wave resonances used to parametrize $F_s(m_{\pi\pi}^2)$ include both the resonant and nonresonant parts of the S-wave two-pion distribution amplitude. Therefore, we take into account $f_0(980)$, $f_0(1500)$ and $f_0(1790)$ in the $s\bar{s}$ density operator, and $f_0(500)$ in the $u\bar{u}$ density operator:

$$F_s^{s\bar{s}}(m_{\pi\pi}^2)=\frac{c_1m_{f_0(980)}^2e^{i\theta_1}}{m_{f_0(980)}^2-m_{\pi\pi}^2-im_{f_0(980)}(g_{\pi\pi}\rho_{\pi\pi}+g_{KK}\rho_{KK})} +\frac{c_2m_{f_0(1500)}^2e^{i\theta_2}}{m_{f_0(1500)}^2-m_{\pi\pi}^2-im_{f_0(1500)}\Gamma_{f_0(1500)}(m_{\pi\pi}^2)} +\frac{c_3m_{f_0(1790)}^2e^{i\theta_3}}{m_{f_0(1790)}^2-m_{\pi\pi}^2-im_{f_0(1790)}\Gamma_{f_0(1790)}(m_{\pi\pi}^2)},$$
$$F_s^{u\bar{u}}(m_{\pi\pi}^2)=\frac{c_0m_{f_0(500)}^2}{m_{f_0(500)}^2-m_{\pi\pi}^2-im_{f_0(500)}\Gamma_{f_0(500)}(m_{\pi\pi}^2)}. \quad (11)$$

c_0, c_i and θ_i, $i=1,2,3$, are tunable parameters. m_S is the pole mass of the resonance, and $\Gamma_S(m_{\pi\pi})$ is the energy dependent width of the S-wave resonance which decays into two pions. For the contribution of $f_0(980)$, an anomalous structure was found around 980 MeV in the $\pi^+\pi^-$ scattering [54, 55]. This was accompanied by the observation of a narrow anomaly (less than 100 MeV wide) in the S-wave phase shift associated with an enhancement in the $(I=0)$ $K\bar{K}$ system at threshold. It was shown that the anomaly could be understood as a narrow two-channel resonance, which combines the $\pi\pi$ and $K\bar{K}$ channels [56]. Generally, the Breit-Wigner (BW) model can be applied to describe an unstable particle as an isolated resonance. Since the resonance $f_0(980)$ is near the threshold of $K\bar{K}$ of about 992 MeV, the model should be modified to include the coupled channels $f_0(980)\to\pi\pi$ and $f_0(980)\to K\bar{K}$ [56]. Therefore, the Breit-Wigner form proposed by Flatté and adopted widely in many studies of the $\pi-\pi$ and $K\bar{K}$ system is also used in this work. In the Flatté model, the phase space factors $\rho_{\pi\pi}$ and ρ_{KK} are given as [48]

$$\begin{aligned}\rho_{\pi\pi} &= \frac{2}{3}\sqrt{1-\frac{4m^2_{\pi^\pm}}{m^2_{\pi\pi}}}+\frac{2}{3}\sqrt{1-\frac{4m^2_{\pi^0}}{m^2_{\pi\pi}}},\\ \rho_{KK} &= \frac{1}{2}\sqrt{1-\frac{4m^2_{K^\pm}}{m^2_{\pi\pi}}}+\frac{1}{2}\sqrt{1-\frac{4m^2_{K^0}}{m^2_{\pi\pi}}}.\end{aligned} \tag{12}$$

3 Perturbative calculations

According to the factorization theorem, the amplitude of a process can be calculated as an expansion in $\alpha_s(Q)$ and Λ/Q, where Q denotes a large momentum transfer, and Λ is a small hadronic scale. Usually, the factorization formula for the nonleptonic b-meson decays can be expressed as

$$\begin{aligned}A\sim &\int_0^1 \mathrm{d}x_1\mathrm{d}x_2\mathrm{d}x_3\int \mathrm{d}^2\boldsymbol{b}_1\mathrm{d}^2\boldsymbol{b}_2\mathrm{d}^2\boldsymbol{b}_3\, C(t)\phi_B(x_1,\boldsymbol{b}_1,t)\\ &\times H(x_1,x_2,x_3,\boldsymbol{b}_1,\boldsymbol{b}_2,\boldsymbol{b}_3,t)\phi_2(x_2,\boldsymbol{b}_2,t)\phi_3(x_3,\boldsymbol{b}_3,t),\end{aligned} \tag{13}$$

where the Wilson coefficients and the typical scale t. The hard kernel $H(x_i,\boldsymbol{b}_i,\boldsymbol{t})$, representing b-quark decay subamplitude, and the nonperturbative meson wave function $\phi_i(x_i,\boldsymbol{b}_i,\boldsymbol{t})$, describe the evolution from scale t to the lower hadronic scale $\Lambda_{\rm QCD}$. For a review of this approach, see Ref. [7].

The effective Hamiltonian for $\bar{B}^0_s\to D^0(\bar{D}^0)\pi^+\pi^-$ is given as

$$\mathcal{H}_{\rm eff}=\frac{G_F}{\sqrt{2}}V_{Qb}V_{qs}(C_1O_1+C_2O_2),\ (Q=c,u,\ q=u,c), \tag{14}$$

with $O_1=(\bar{c}_\alpha b_\beta)_{V-A}(\bar{s}_\beta u_\alpha)_{V-A}$, $O_2=(\bar{c}_\alpha b_\alpha)_{V-A}(\bar{s}_\beta u_\beta)_{V-A}$ for the $\bar{B}^0_s\to D^0\pi^+\pi^-$ process, and $O_1=(\bar{u}_\alpha b_\beta)_{V-A}(\bar{s}_\beta c_\alpha)_{V-A}$, $O_2=(\bar{u}_\alpha b_\alpha)_{V-A}(\bar{s}_\beta c_\beta)_{V-A}$ for the process $\bar{B}^0_s\to\bar{D}^0\pi^+\pi^-$. In particular, the penguin operators do not contribute to the processes. Using the above effective Hamiltonian, we obtain the typical Feynman diagrams for the $\bar{B}^0_s\to D^0\pi^+\pi^-$ process shown in Fig. 1, in which the first row represents the color-suppressed emission process, and the second row indicates the W-exchange process. In the factorization framework, the factorizable diagrams in Fig. 1 (a,b,e,f) are relevant for a_2, and the non-factorizable diagrams in Fig. 1 (c,d,g,h) are proportional to C_2 [57], where

$$a_1=C_2+C_1/N_c,\quad a_2=C_1+C_2/N_c. \tag{15}$$

We will work in the light-cone coordinates. The momenta of the mesons are defined as follows:

$$\begin{aligned}P_{B_s} &=(p_1^+,p_1^-,0_\perp),\quad P_{\pi\pi}=(p_2^+,0,0_\perp),\\ P_D &=(p_1^+-p_2^+,m^2_{B_s}/(2p_1^+),0_\perp).\end{aligned} \tag{16}$$

Accordingly, the momentum transfer and the light-cone components can be obtained as $q^2=(P_{B_s}-P_{\pi\pi})^2=(1-\rho)m^2_{B_s}$, $\rho=1-\dfrac{m_D}{m_{B_s}}$, $p_1^-=m^2_{B_s}/(2p_1^+)$ and $p_2^+=(m^2_{B_s}-q^2)p_1^+/m^2_{B_s}$. In the heavy quark limit, the mass difference between b-quark (c-quark) and $B_s(D)$ meson is negligible, $m_{B_s,D}=m_{b,c}+\bar{\Lambda}$($\bar{\Lambda}$ is of the order of the QCD scale). Since $m_{B_s}\gg m_D\gg\bar{\Lambda}$, we expand the amplitudes in terms of $\dfrac{m_D}{m_{B_s}}$, $\dfrac{\bar{\Lambda}}{m_D}$, and for high order $\dfrac{\bar{\Lambda}}{m_{B_s}}$. For the leading order of the expansion, $\rho\sim1, q^2\sim0$. The momenta of the light quarks in the mesons (k_1,k_3 represent the momenta of the light quarks in B_s and D mesons, k_2 is the momentum of the positive quark in the pion-pair system) are given as

$$k_1=(0,x_1P^-_{B_s},k_{1\perp}),\ k_2=(x_2P^+_{\pi\pi},0,k_{2\perp}),\ k_3=(0,x_3P^-_D,k_{3\perp}). \tag{17}$$

In the k_T-factorization, the color-suppressed emission Feynman diagrams can be calculated out, with the formulas labeled as e_x (x = 1,2,3,4) in the subscript. Thus, the factorization formulas for the color-suppressed D^0-emission diagrams are given as

$$\begin{aligned}\mathcal{M}_{e12} =& 8\pi C_F m^4_{B_s} f_D\int_0^1 \mathrm{d}x_1\mathrm{d}x_2\int_0^{1/\Lambda} b_1\mathrm{d}b_1 b_2\mathrm{d}b_2\phi_B(x_1,b_1)\\ &\times\{E_{e_1}(t_{e_1})h_{e_1}(x_1,x_2,b_1,b_2)a_2(t_{e_1})\\ &\times[r_0(1-2x_2)(\phi^s_{\pi\pi}(s\bar{s},x_2)-\phi^T_{s\bar{s},\pi\pi}(x_2))\\ &+(2-x_2)\phi_{\pi\pi}(s\bar{s},x_2)]-2r_0\phi^s_{\pi\pi}(s\bar{s},x_2)\\ &\times E_{e_2}(t_{e_2})h_{e_2}(x_1,x_2,b_1,b_2)a_2(t_{e_2})\},\\ \mathcal{M}_{e34} =& \frac{32\pi C_F m^4_{B_s}}{\sqrt{2N_c}}\int_0^1 \mathrm{d}x_1\mathrm{d}x_2\mathrm{d}x_3\int_0^{1/\Lambda} b_1\mathrm{d}b_1 b_3\mathrm{d}b_3\phi_B(x_1,b_1)\\ &\times\phi_D(\bar{x}_3,b_3)C_2(t_{e_3})\{E_{e_3}(t_{e_3})h_{e_3}(x_1,x_2,x_3,b_1,b_3)\\ &\times[r_0\bar{x}_2(\phi^s_{\pi\pi}(s\bar{s},x_2)+\phi^T_{\pi\pi}(s\bar{s},x_2))+x_3\phi_{\pi\pi}(s\bar{s},x_2)]\\ &-E_{e_4}(t_{e_4})h_{e_4}(x_1,x_2,x_3,b_1,b_3)[r_0\bar{x}_2(\phi^s_{\pi\pi}(s\bar{s},x_2)\\ &-\phi^T_{\pi\pi}(s\bar{s},x_2))+(\bar{x}_3+\bar{x}_2)\phi_{\pi\pi}(s\bar{s},x_2)]\},\end{aligned} \tag{18}$$

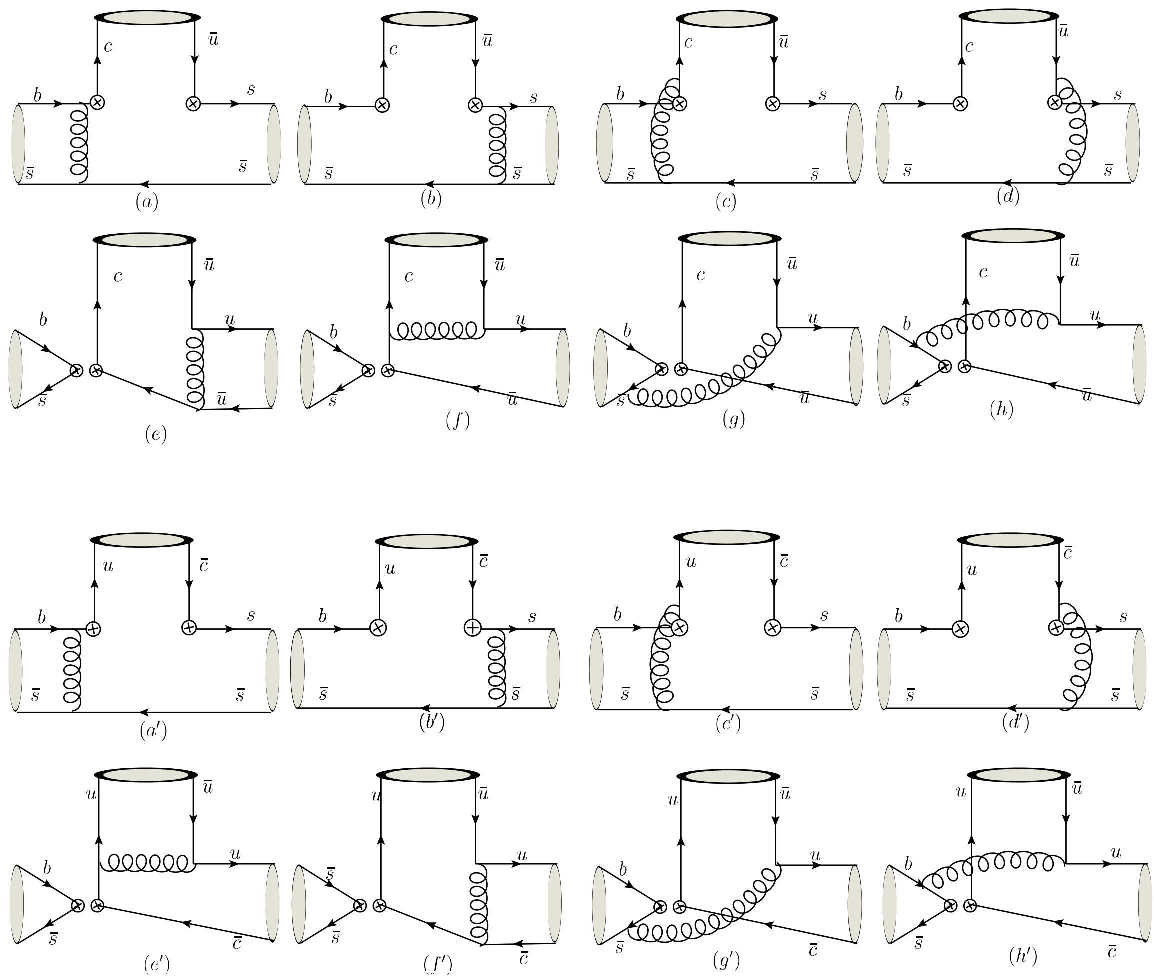

Fig. 1. (color online) Typical Feynman diagrams for the three-body decays $\bar{B}_s^0 \to D^0(\bar{D}^0)\pi^+\pi^-$. For the three-body process, the operators at the quark level are O_1,O_2, which correspond to two kinds of Feynman diagrams: the color-suppressed and the W-exchange. The color-suppressed diagrams are shown in panels (*a-d*) and (*a*'-*d*'); the W-exchange diagrams are shown in panels (*e-h*) and (*e*'-*h*').

where $r_0 = \frac{m_{\pi\pi}}{m_{B_s}}$, C_F is the color factor. $\phi_{\pi\pi}(s\bar{s}, x_2)$ represents the two-pion distribution amplitude defined by the $s\bar{s}$ operator. The hard kernels E_{e_x} and h_{e_x} are given in the following.

The factorization formulas for the W-exchange D^0 diagrams $\mathcal{M}_{w12}$ and $\mathcal{M}_{w34}$ are given as

$$\begin{aligned}\mathcal{M}_{w12} =& 8\pi C_F m_{B_s}^4 f_{B_s} \int_0^1 \mathrm{d}x_2 \mathrm{d}x_3 \int_0^{1/\Lambda} b_2 \mathrm{d}b_2 b_3 \mathrm{d}b_3 \phi_D(x_3, b_3) \\ &\times \{E_{w_1}(t_{w_1}) h_{w_1}(x_2, x_3, b_2, b_3) a_2(t_{w_1}) [x_3 \phi_{\pi\pi}(u\bar{u}, x_2) \\ &+ 2 r_0 r_D (x_3+1) \phi_{\pi\pi}^s(u\bar{u}, x_2)] - [x_2 \phi_{\pi\pi}(u\bar{u}, x_2) \\ &- r_0 r_D (2x_2+1) \phi_{\pi\pi}^s(u\bar{u}, x_2) + r_0 r_D (1-2x_2) \phi_{\pi\pi}^T(u\bar{u}, x_2)] \\ &\times E_{w_2}(t_{w_2}) h_{w_2}(x_2, x_3, b_2, b_3) a_2(t_{w_2})\},\end{aligned}$$

$$\begin{aligned}\mathcal{M}_{w34} =& \frac{32\pi C_F m_{B_s}^4}{\sqrt{2N_c}} \int_0^1 \mathrm{d}x_1 \mathrm{d}x_2 \mathrm{d}x_3 \int_0^{1/\Lambda} b_1 \mathrm{d}b_1 b_2 \mathrm{d}b_2 \phi_{B_s}(x_1, b_1) \\ &\times \phi_D(x_3, b_2) \{E_{w_3}(t_{w_3}) h_{w_3}(x_1, x_2, x_3, b_1, b_2) C_2(t_{w_3}) \\ &\times [x_2 \phi_{\pi\pi}(u\bar{u}, x_2) + r_0 r_D (x_2+x_3) \phi_{\pi\pi}^s(u\bar{u}, x_2) \\ &+ r_0 r_D (x_2-x_3) \phi_{\pi\pi}^T(u\bar{u}, x_2)] + [-x_3 \phi_{\pi\pi}(u\bar{u}, x_2) \\ &- r_0 r_D (x_2+x_3+2) \phi_{\pi\pi}^s(u\bar{u}, x_2) + r_0 r_D (x_2-x_3) \\ &\times \phi_{\pi\pi}^T(u\bar{u}, x_2)] E_{w_4}(t_{w_4}) h_{w_4}(x_1, x_2, x_3, b_1, b_2) C_2(t_{w_4})\}, \quad (19)\end{aligned}$$

where $r_D = \frac{m_D}{m_{B_s}}$, $\phi_{\pi\pi}(u\bar{u}, x_2)$ represents the distribution amplitude of the $u\bar{u}$ operator. Due to the helicity suppression, the contribution of the factorizable diagrams $\mathcal{M}_{w12}$ is suppressed significantly. Therefore, the dominant contribution comes from the non-factorizable diagrams $\mathcal{M}_{w34}$.

In the $\bar{D}^0$-emission process, the two factorizable diagrams have the same factorization $\mathcal{M}_{e12} = \mathcal{M}_{e'12}$. Accordingly, we give the factorization formulas for the non-factorizable emission diagrams $\mathcal{M}_{e'34}$, the factorizable W-exchange diagrams $\mathcal{M}_{w'12}$ and the non-factorizable W-exchange diagrams $\mathcal{M}_{w'34}$ as follows:

$$\begin{aligned}
\mathcal{M}_{e'34} =& \frac{32\pi C_F m_{B_s}^4}{\sqrt{2N_c}}\int_0^1 \mathrm{d}x_1\mathrm{d}x_2\mathrm{d}x_3\int_0^{1/\Lambda} b_1\mathrm{d}b_1 b_3\mathrm{d}b_3\phi_B(x_1,b_1)\\
&\times\phi_D(\bar{x}_3,b_3)\{E_{e'_3}(t_{e'_3})h_{e'_3}(x_1,x_2,x_3,b_1,b_3)C_2(t_{e'_3})\\
&\times[r_0(\bar{x}_2)(\phi^s_{\pi\pi}(s\bar{s},x_2)+\phi^T_{\pi\pi}(s\bar{s},x_2))+x_3\phi_{\pi\pi}(s\bar{s},x_2)]\\
&-E_{e'_4}(t_{e'_4})h_{e'_4}(x_1,x_2,x_3,b_1,b_3)C_2(t_{e'_4})[r_0\bar{x}_2(\phi^s_{\pi\pi}(s\bar{s},x_2)\\
&-\phi^T_{\pi\pi}(s\bar{s},x_2))+(\bar{x}_3+\bar{x}_2)\phi_{\pi\pi}(s\bar{s},x_2)]\},\\
\mathcal{M}_{w'12} =& 8\pi C_F m_{B_s}^4 f_{B_s}\int_0^1 \mathrm{d}x_2\mathrm{d}x_3\int_0^{1/\Lambda} b_2\mathrm{d}b_2 b_3\mathrm{d}b_3\phi_{\bar{D}}(x_3,b_3)\\
&\times\{E_{w'_1}(t_{w'_1})h_{w'_1}(x_2,x_3,b_2,b_3)a_2(t_{w'_1})\\
&\times[(1-x_2)\phi_{\pi\pi}(u\bar{u},x_2)+r_0r_D(2x_2-3)\phi^s_{\pi\pi}(u\bar{u},x_2)\\
&+r_0r_D(1-2x_2)\phi^T_{\pi\pi}(u\bar{u},x_2)]+[-x_3\phi_{\pi\pi}(u\bar{u},x_2)\\
&+2r_0r_D(x_3+1)\phi^s_{\pi\pi}(u\bar{u},x_2)]E_{w'_2}(t_{w'_2})\\
&\times h_{w'_2}(x_2,x_3,b_2,b_3)a_2(t_{w'_2})\},\\
\mathcal{M}_{w'34} =& \frac{32\pi C_F m_{B_s}^4}{\sqrt{2N_c}}\int_0^1 \mathrm{d}x_1\mathrm{d}x_2\mathrm{d}x_3\int_0^{1/\Lambda} b_1\mathrm{d}b_1 b_2\mathrm{d}b_2\phi_{B_s}(x_1,b_1)\\
&\times\phi_{\bar{D}}(x_3,b_2)\{E_{w'_3}(t_{w'_3})h_{w'_3}(x_1,x_2,x_3,b_1,b_2)C_2(t_{w'_3})\\
&\times[x_3\phi_{\pi\pi}(u\bar{u},x_2)-r_0r_D(1-x_2+x_3)\phi^s_{\pi\pi}(u\bar{u},x_2)\\
&+r_0r_D(x_2+x_3-1)\phi^T_{\pi\pi}(u\bar{u},x_2)]+[(x_2-1)\phi_{\pi\pi}(u\bar{u},x_2)\\
&+r_0r_D(-x_2+x_3+3)\phi^s_{\pi\pi}(u\bar{u},x_2)+r_0r_D(x_2+x_3-1)\\
&\times\phi^T_{\pi\pi}(u\bar{u},x_2)]E_{w'_4}(t_{w'_4})h_{w'_4}(x_1,x_2,x_3,b_1,b_2)C_2(t_{w'_4})\}.
\end{aligned}\tag{20}$$

In the following, we give the forms for the offshellness of the intermediate gluon β_{e_x}/β_{w_x} and quarks $\alpha_{e_x}/\alpha_{w_x}(x=1,2,3,4)$ in the $\bar{B}^0_s\to D^0\pi^+\pi^-$ process.

$$\begin{aligned}
\alpha_{e_1} =&(1-x_2)m_{B_s}^2\rho,\ \ \alpha_{e_2}=x_1m_{B_s}^2\rho,\\
\alpha_{e_3} =&x_1(1-x_2)m_{B_s}^2\rho,\ \ \alpha_{e_4}=x_1(1-x_2)m_{B_s}^2\rho,\\
\alpha_{w_1} =&x_3m_{B_s}^2\rho,\ \ \alpha_{w_2}=(1-\rho+x_2\rho)m_{B_s}^2,\\
\alpha_{w_3} =&x_2x_3m_{B_s}^2\rho,\ \ \alpha_{w_4}=x_2x_3m_{B_s}^2\rho,\\
\beta_{e_1} =&x_1(1-x_2)m_{B_s}^2\rho,\ \ \beta_{e_2}=x_1(1-x_2)m_{B_s}^2\rho,\\
\beta_{e_3} =&[(x_1-x_3)(1-x_2\rho)+(1-\rho)]m_{B_s}^2,\\
\beta_{e_4} =&(1-x_2)(x_1+x_3-1)m_{B_s}^2\rho,\\
\beta_{w_1} =&x_2x_3m_{B_s}^2\rho,\ \ \beta_{w_2}=x_2x_3m_{B_s}^2\rho,\\
\beta_{w_3} =&(x_3-x_1)x_2m_{B_s}^2\rho,\\
\beta_{w_4} =&((1-x_1-x_3)(1-x_2\rho)-1)m_{B_s}^2.
\end{aligned}\tag{21}$$

For $B^0_s\to\bar{D}^0\pi^+\pi^-$, we have

$$\begin{aligned}
\alpha_{e'_1} =&(1-x_2)m_{B_s}^2\rho,\ \ \alpha_{e'_2}=x_1m_{B_s}^2\rho,\\
\alpha_{e'_3} =&x_1(1-x_2)m_{B_s}^2\rho,\ \ \alpha_{e'_4}=x_1(1-x_2)m_{B_s}^2\rho,\\
\alpha_{w'_1} =&(1-x_2\rho)m_{B_s}^2,\ \ \alpha_{w'_2}=x_3m_{B_s}^2\rho,\\
\alpha_{w'_3} =&x_3(1-x_2)m_{B_s}^2\rho,\ \ \alpha_{w'_4}=x_3(1-x_2)m_{B_s}^2\rho,\\
\beta_{e'_1} =&x_1(1-x_2)m_{B_s}^2\rho,\ \ \beta_{e'_2}=x_1(1-x_2)m_{B_s}^2\rho,\\
\beta_{e'_3} =&(1-x_2)(x_1-x_3)m_{B_s}^2\rho,\\
\beta_{e'_4} =&[(x_1+x_3-1)(1-x_2\rho)+(1-\rho)]m_{B_s}^2,\\
\beta_{w'_1} =&x_3(1-x_2)m_{B_s}^2\rho,\ \ \beta_{w'_2}=x_3(1-x_2)m_{B_s}^2\rho,\\
\beta_{w'_3} =&(1-x_2)(x_3-x_1)m_{B_s}^2\rho,\\
\beta_{w'_4} =&((1-x_1-x_3)(1-\rho+x_2\rho)-1)m_{B_s}^2.
\end{aligned}\tag{22}$$

The hard kernel functions $h_{e_x}(h_{e'_x})$ and $h_{w_x}(h_{w'_x})$ are written as

$$\begin{aligned}
h_{e_i}(x_1,x_2,b_1,b_2) =&[\theta(b_1-b_2)I_0(\sqrt{\alpha_{e_i}}b_2)K_0(\sqrt{\beta_{e_i}}b_1)+(b_1\leftrightarrow b_2)]K_0(\sqrt{\beta_{e_i}}b_1)S_t(\alpha_{e_i}/(m_{B_s}^2\rho)),\\
h_{e_j}(x_1,x_2,x_3,b_1,b_3) =&[\theta(b_1-b_3)I_0\left(\sqrt{\alpha_{e_j}}b_3\right)K_0\left(\sqrt{\beta_{e_j}}b_1\right)+(b_1\leftrightarrow b_3)]\begin{cases}K_0\left(\sqrt{\beta_{e_j}}b_1\right), & \beta_{e_j}\geqslant 0,\\ \frac{i\pi}{2}H_0^{(1)}\left(\sqrt{|\beta_{e_j}|}b_1\right), & \beta_{e_j}<0,\end{cases},\\
h_{w_k}(x_1,x_2,b_2,b_3) =&\left(i\frac{\pi}{2}\right)^2H_0^{(1)}(\sqrt{\beta_{w_k}}b_2)[\theta(b_2-b_3)H_0^{(1)}(\sqrt{\alpha_{w_k}}b_2)J_0(\sqrt{\alpha_{w_k}}b_3)+(b_2\leftrightarrow b_3)]S_t(\alpha_{w_k}/(m_{B_s}^2\rho)),\\
h_{w_l}(x_1,x_2,x_3,b_1,b_2) =&i\frac{\pi}{2}[\theta(b_1-b_2)H_0^{(1)}(\sqrt{\alpha_{w_l}}b_1)J_0(\sqrt{\alpha_{w_l}}b_2)+(b_1\leftrightarrow b_2)]\begin{cases}K_0(\sqrt{\beta_{w_l}}b_1), & \beta_{w_l}\leqslant 0,\\ \frac{i\pi}{2}H_0^{(1)}(\sqrt{|\beta_{w_l}|}b_1), & \beta_{w_l}>0,\end{cases}.
\end{aligned}\tag{23}$$

where $i,k=1,2$ and $j,l=3,4$, and I_0, K_0 and $H_0=J_0+iY_0$ are the Bessel functions. The threshold re-summation factor $S_t(x)$ is parametrized as

$$S_t(x)=\frac{2^{1+2c}\Gamma(3/2+c)}{\sqrt{\pi}\Gamma(1+c)}[x(1-x)]^c,\tag{24}$$

with the parameter $c=0.4$ in this work. The evolution factors $E_x(t)$ in the factorization formulas are given by

$$\begin{aligned}
E_{e_i}(t) =&\alpha_s(t)\exp(-S_{B_s}(t)-S_{\pi\pi}(t)),\\
E_{e_j}(t) =&\alpha_s(t)\exp(-S_{B_s}(t)-S_{\pi\pi}(t)-S_D(t))|_{b_1=b_2},\\
E_{w_k}(t) =&\alpha_s(t)\exp(-S_{\pi\pi}(t)-S_D(t)),\\
E_{w_l}(t) =&\alpha_s(t)\exp(-S_{B_s}(t)-S_{\pi\pi}(t)-S_D(t))|_{b_2=b_3},
\end{aligned}\tag{25}$$

where

$$S_{B_s}(t)=s(x_1m_{B_s},b_1)+\frac{5}{3}\int_{1/b_1}^t\frac{\mathrm{d}\bar{\mu}}{\bar{\mu}}\gamma_q(\alpha_s(\bar{\mu})),$$

$$S_D(t)=s(x_3 m_{B_s},b_3)+2\int_{1/b_3}^{t}\frac{d\bar{\mu}}{\bar{\mu}}\gamma_q(\alpha_s(\bar{\mu})),$$
$$S_{\pi\pi}(t)=s(x_2 m_{B_s},b_2)+s((1-x_2)m_{B_s},b_2)+2\int_{1/b_2}^{t}\frac{d\bar{\mu}}{\bar{\mu}}\gamma_q(\alpha_s(\bar{\mu})), \quad (26)$$

with the quark anomalous dimension $\gamma_q=-\alpha_s/\pi$. The explicit expression for $s(Q,b)$ can be found, for example, in Appendix A of Ref. [9]. The hard scales are chosen as

$$t_{e_i}=\max(\sqrt{\alpha_{e_i}},\sqrt{\beta_{e_i}},1/b_1,1/b_2),$$
$$t_{e_j}=\max(\sqrt{\alpha_{e_j}},\sqrt{\beta_{e_j}},1/b_1,1/b_3),$$
$$t_{w_k}=\max(\sqrt{\alpha_{w_k}},\sqrt{\beta_{w_k}},1/b_2,1/b_3),$$
$$t_{w_l}=\max(\sqrt{\alpha_{w_l}},\sqrt{\beta_{w_l}},1/b_1,1/b_2). \quad (27)$$

Therefore, we obtain the total decay amplitudes,

$$\mathcal{A}(\bar{B}_s\to D^0\pi^+\pi^-)=\frac{G_F}{\sqrt{2}}V_{cb}V_{us}^*(\mathcal{M}_{e12}+\mathcal{M}_{e34}+\mathcal{M}_{w12}+\mathcal{M}_{w34}),$$
$$\mathcal{A}(\bar{B}_s\to \bar{D}^0\pi^+\pi^-)=\frac{G_F}{\sqrt{2}}V_{ub}V_{cs}^*(\mathcal{M}_{e'12}+\mathcal{M}_{e'34}+\mathcal{M}_{w'12}+\mathcal{M}_{w'34}). \quad (28)$$

The differential branching ratio for the decays $\bar{B}_s^0\to D^0(\bar{D}^0)\pi^+\pi^-$ follows the formula given in [58, 59]

$$\frac{d\mathcal{B}}{dm_{\pi\pi}}=\tau_{B_s}\frac{m_{\pi\pi}|\overrightarrow{p_1}||\overrightarrow{p_3}|}{4(2\pi)^3 m_{B_s}^3}|\mathcal{A}|^2, \quad (29)$$

with the B_s meson mean lifetime τ_{B_s}. The kinematic variables $|\overrightarrow{p_1}|$ and $|\overrightarrow{p_3}|$ denote the magnitudes of the π^+ and D momenta in the center-of-mass frame of the pion pair,

$$|\overrightarrow{p_1}|=\frac{1}{2}\sqrt{m_{\pi\pi}^2-4m_{\pi^\pm}^2},$$
$$|\overrightarrow{p_3}|=\frac{1}{2m_{\pi\pi}}\sqrt{\left[m_{B_s}^2-(m_{\pi\pi}+m_D)^2\right]\left[m_{B_s}^2-(m_{\pi\pi}-m_D)^2\right]}. \quad (30)$$

4 Numerical results

We adopt the following inputs (in units of GeV) [58, 59]

$$\Lambda_{\overline{MS}}^{f=4}=0.250,\ m_{B_s}=5.367,\ m_{D^0}=1.869,\ m_{\pi^\pm}=0.140,$$
$$m_{\pi^0}=0.135,\ m_{K^\pm}=0.494,$$
$$m_{K^0}=0.498,\ m_b=4.66,\ m_s=0.095,$$
$$\tau_{B_s}=1.512\times10^{-12}s,\ G_F=1.166\times10^{-5},$$

and the CKM matrix elements are taken as:

$$|V_{us}|=0.2252,\ |V_{ub}|=3.89\times10^{-3},$$
$$|V_{cs}|=0.97345,\ |V_{cb}|=40.6\times10^{-3}.$$

The parameters of the scalar form factor $F_s(m_{\pi\pi}^2)$ are extracted from the LHCb data for the process $B_s\to J/\psi\pi^+\pi^-$, given in [48, 60] (mass and widths are given in units of GeV):

$$m(f_0(500))=0.5,\ m(f_0(980))=0.97,$$
$$m(f_0(1500))=1.5,\ m(f_0(1790))=1.81,$$
$$\Gamma(f_0(500))=0.4,\ \Gamma(f_0(1500))=0.12,\ \Gamma(f_0(1790))=0.32,$$
$$g_{\pi\pi}=0.167,\ g_{KK}=3.47g_{\pi\pi},$$
$$c_0=3.500,\ c_1=0.900,\ c_2=0.106,\ c_3=0.066,$$
$$\theta_1=-\frac{\pi}{2},\ \theta_2=\frac{\pi}{4},\ \theta_3=0.$$

We calculate the branching ratios for the different resonances in the S-wave pion-pair wave function, which are given in Table 1. In this table, the first uncertainties are from $\omega_b=0.50\pm0.05$ in the B_s wave function, the second arise from $a_2=0.2\pm0.2$ in the pion-pair wave function, and the third are from the QCD scale $\Lambda=0.25\pm0.05$. The errors from the parameter C_D in the D meson wave function, the variations of the CKM matrix elements and the mean lifetime of B_s are small and have been omitted. However, the above results are sensitive to ω_b and a_2, namely the B_s and S-wave two-pion wave functions. Future measurements of decay branching ratios will be valuable for understanding B_s physics and the S-wave two-pion resonances.

Including all S-wave resonances $f_0(500)$, $f_0(980)$, $f_0(1500)$ and $f_0(1790)$ in the scalar form factor, we obtain the total branching ratio

Table 1. Branching ratios from the different intermediate resonances.

Resonances	Branching ratio ($\times10^{-6}$)
$\bar{B}_s^0\to D^0 f_0(500)[f_0(500)\to\pi^+\pi^-]$	$0.13^{+0.04}_{-0.03}(\omega_b)^{+0.19}_{-0.09}(a_2)^{+0.04}_{-0.01}(\Lambda_{\rm QCD})$
$\bar{B}_s^0\to D^0 f_0(980)[f_0(980)\to\pi^+\pi^-]$	$0.45^{+0.12}_{-0.12}(\omega_b)^{+0.53}_{-0.13}(a_2)^{+0.09}_{-0.11}(\Lambda_{\rm QCD})$
$\bar{B}_s^0\to D^0 f_0(1500)[f_0(1500)\to\pi^+\pi^-]$	$0.11^{+0.04}_{-0.03}(\omega_b)^{+0.08}_{-0.02}(a_2)^{+0.02}_{-0.03}(\Lambda_{\rm QCD})$
$\bar{B}_s^0\to D^0 f_0(1790)[f_0(1790)\to\pi^+\pi^-]$	$0.035^{+0.012}_{-0.010}(\omega_b)^{+0.017}_{-0.003}(a_2)^{+0.007}_{-0.008}(\Lambda_{\rm QCD})$
$\bar{B}_s^0\to \bar{D}^0 f_0(500)[f_0(500)\to\pi^+\pi^-]$	$0.11^{+0.05}_{-0.04}(\omega_b)^{+0.22}_{-0.09}(a_2)^{+0.00}_{-0.02}(\Lambda_{\rm QCD})$
$\bar{B}_s^0\to \bar{D}^0 f_0(980)[f_0(980)\to\pi^+\pi^-]$	$0.16^{+0.06}_{-0.05}(\omega_b)^{+0.17}_{-0.11}(a_2)^{+0.01}_{-0.01}(\Lambda_{\rm QCD})$
$\bar{B}_s^0\to \bar{D}^0 f_0(1500)[f_0(1500)\to\pi^+\pi^-]$	$0.039^{+0.014}_{-0.013}(\omega_b)^{+0.031}_{-0.022}(a_2)^{+0.001}_{-0.001}(\Lambda_{\rm QCD})$
$\bar{B}_s^0\to \bar{D}^0 f_0(1790)[f_0(1790)\to\pi^+\pi^-]$	$0.011^{+0.004}_{-0.003}(\omega_b)^{+0.008}_{-0.006}(a_2)^{+0.000}_{-0.000}(\Lambda_{\rm QCD})$

$$\mathcal{B}(\bar{B}_s^0 \to D^0(\pi^+\pi^-)_S) = 0.77^{+0.19}_{-0.18}(\omega_b)^{+1.00}_{-0.28}(a_2)^{+0.11}_{-0.12} \times (\Lambda_{\rm QCD}) \times 10^{-6},$$
$$\mathcal{B}(\bar{B}_s^0 \to \bar{D}^0(\pi^+\pi^-)_S) = 0.47^{+0.19}_{-0.15}(\omega_b)^{+0.60}_{-0.33}(a_2)^{+0.02}_{-0.05} \times (\Lambda_{\rm QCD}) \times 10^{-6}. \quad (31)$$

We found the contributions of $\bar{B}_s^0 \to D^0 f_0(500)[f_0(500) \to \pi^+\pi^-]$, $\bar{B}_s^0 \to D^0 f_0(980)[f_0(980) \to \pi^+\pi^-]$, $\bar{B}_s^0 \to D^0 f_0(1500)[f_0(1500) \to \pi^+\pi^-]$ and $\bar{B}_s^0 \to D^0 f_0(1790)[f_0(1790) \to \pi^+\pi^-]$ to be respectively 16.4%, 59.3%, 14.6% and 4.5% of the total $\bar{B}_s^0 \to D^0(\pi^+\pi^-)_S$ decay rate. For the $\bar{B}_s^0 \to \bar{D}^0(\pi^+\pi^-)_S$ process, the corresponding rates are respectively 24.6%, 35.2%, 8.3% and 2.4% . This indicates that the $f_0(500)$ and $f_0(980)$ contributions are dominant, and that the contribution from $f_0(980)$ is larger than $f_0(500)$ in the $D^0(\bar{D}^0)$ final state. LHCb collaboration measured the upper limit of the branching ratio of $\mathcal{B}(B_s \to \bar{D}^0 f_0(980)) < 3.1 \times 10^{-6}$ [61], which roughly agrees with our value.

In order to compare the two channels $\bar{B}_s \to D^0(\pi\pi)_S$ and $\bar{B}_s \to \bar{D}^0(\pi\pi)_S$, we determine the rate of their branching ratios

$$R_1 = \frac{\mathcal{B}(\bar{B}_s^0 \to D^0(\pi^+\pi^-)_S)}{\mathcal{B}(\bar{B}_s^0 \to \bar{D}^0(\pi^+\pi^-)_S)} \sim 1.64, \quad (32)$$

which significantly deviates from the ratio of the CKM factors:

$$R_{\rm CKM} = |\frac{V_{cb}V_{us}^*}{V_{ub}V_{cs}^*}| \sim 5.83. \quad (33)$$

In these two decays, there are competition effects from the CKM factors and dynamical decay amplitudes. In these processes, the dominant contributions come from the emission diagrams and non-factorizable W-exchange diagrams. Although the emission diagrams result in similar factorization formulas and numerical results for the two channels, the formulas for the non-factorizable W-exchange diagrams are different. We found that the non-factorizable W-exchange process for $\bar{B}_s^0 \to \bar{D}^0\pi^+\pi^-$ is numerically larger than for $\bar{B}_s^0 \to D^0\pi^+\pi^-$, with the CKM factor inversed. As a result, their final branching ratios are similar.

The CKM element for $\bar{B}_s^0 \to D^0(\bar{D}^0)(\pi^+\pi^-)_S$ is $V_{cb}V_{us}^*$ ($V_{ub}V_{cs}^*$), where V_{ub} is sensitive to γ. Therefore, we can get the dependence of our results on γ by providing a parameter $D_{\rm CP\pm}$ defined as [62]

$$\sqrt{2}\mathcal{A}(\bar{B}_s^0 \to D_{\rm CP\pm}(\pi^+\pi^-)_S) = \mathcal{A}(\bar{B}_s^0 \to D^0(\pi^+\pi^-)_S) \pm \mathcal{A}(\bar{B}_s^0 \to \bar{D}^0(\pi^+\pi^-)_S). \quad (34)$$

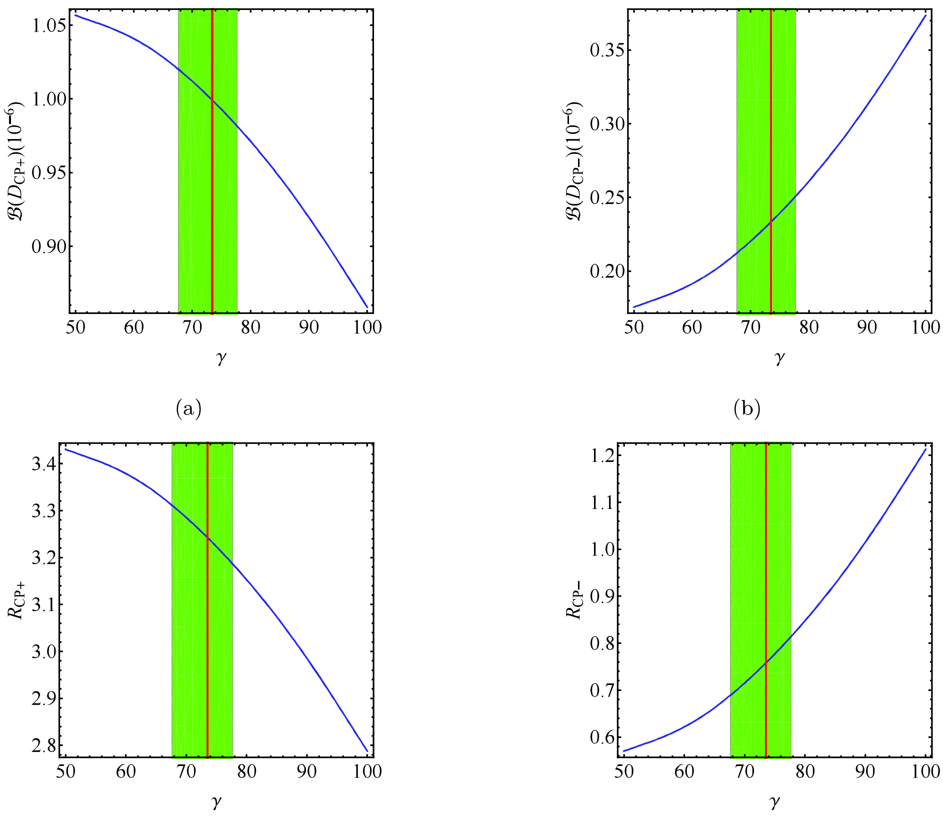

Fig. 2. (color online) The dependence of the differential branching ratios $\mathcal{B}(\bar{B}_s^0 \to D_{\rm CP\pm}(\pi^+\pi^-)_S)$ on γ are shown in panels (a,b). In panels (c,d), the corresponding physical observable that is measured $R_{\rm CP\pm}$ is shown as function of γ. The shaded (green) regions denote the current bound $\gamma = 73.5^{+4.2}_{-5.9}$.

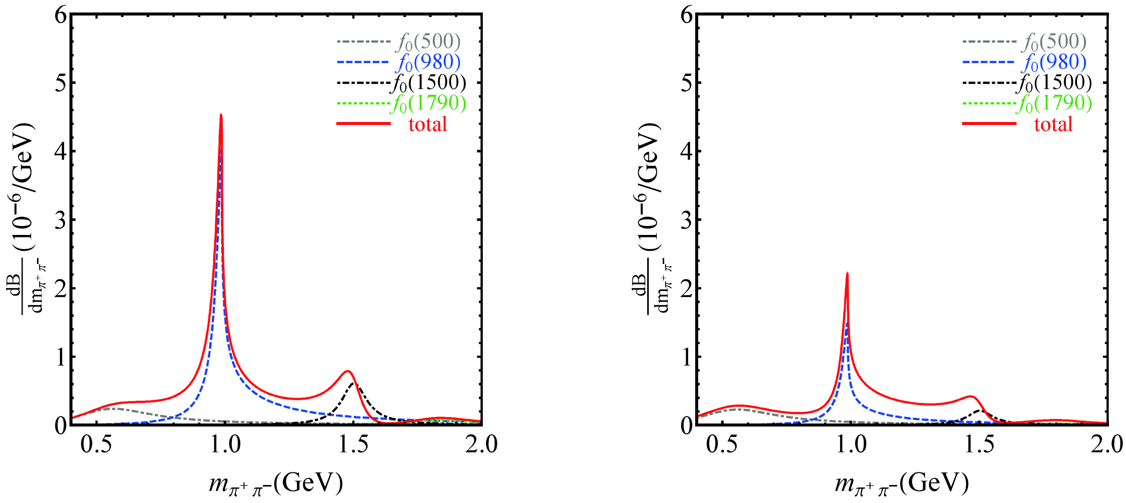

(a) (b)

Fig. 3. (color online) The dependence of the differential branching ratio on the pion-pair invariant mass for the resonances $f_0(980)$, $f_0(1500)$ and $f_0(1790)$ in the decays (a) $\bar{B}_s^0 \to D^0\pi^+\pi^-$ and (b) $\bar{B}_s^0 \to \bar{D}^0\pi^+\pi^-$.

Accordingly, the dependence of the branching ratio $\mathcal{B}(\bar{B}_s^0 \to D_{\mathrm{CP}\pm}(\pi^+\pi^-)_S)$ on γ is shown in Fig. 2(a,b). The corresponding physical observable measured by the experiments is defined as

$$R_{\mathrm{CP}\pm} = \frac{4\mathcal{B}(\bar{B}_s^0 \to D_{\mathrm{CP}\pm}(\pi^+\pi^-)_S)}{\mathcal{B}(\bar{B}_s^0 \to D^0(\pi^+\pi^-)_S) + \mathcal{B}(\bar{B}_s^0 \to \bar{D}^0(\pi^+\pi^-)_S)}. \quad (35)$$

The dependence of $R_{\mathrm{CP}\pm}$ on γ is shown in Fig. 2(c,d). The current bound for γ is $\gamma = (73.5^{+4.2}_{-5.9})^\circ$ [63].

The predicted dependence of the differential branching ratio $\mathrm{d}\mathcal{B}/\mathrm{d}m_{\pi\pi}$ on the pion-pair invariant mass $m_{\pi\pi}$ is presented in Fig. 3(a) and Fig. 3(b) for the resonances $f_0(500)$, $f_0(980)$, $f_0(1500)$ and $f_0(1790)$ in the decays $\bar{B}_s \to D^0\pi^+\pi^-$ and $\bar{B}_s \to \bar{D}^0\pi^+\pi^-$. The figures show that the main contribution to the two decays lies in the region around the pole mass $m_{f_0(980)} = 0.97$, while $f_0(500)$ gives a contribution primarily in the region below $m_{\pi\pi} = 1$ GeV. The other resonances, $f_0(1500)$ and $f_0(1790)$, still give considerable contributions to the processes. Therefore, we hope that more precise data from LHCb and the future KEKB may test our theoretical calculations.

5 Conclusions

In the past decades, two-body B decays have provided an ideal platform for extracting the Standard Model parameters, and for probing new physics beyond SM [64, 65]. In this work, we studied the three-body decays $\bar{B}_s^0 \to D^0(\bar{D}^0)\pi^+\pi^-$ within the PQCD framework, and in particular the S-wave contribution which was explicitly calculated. The S-wave two-pion light-cone distribution amplitudes can have both resonant $f_0(500)$, $f_0(980)$, $f_0(1500)$, $f_0(1790)$ and nonresonant contributions. Furthermore, the processes proceed via tree level operators, and the branching ratios were found to be in the range from 10^{-7} to 10^{-6}. It was found that the branching ratios are sensitive to the parameters ω_b and a_2 in the B_s and two-pion distribution amplitudes. Therefore, we expect that future measurement could help to better understand the multi-body processes and the S-wave two-pion resonance and B_s distribution amplitudes.

References

1 R. Aaij et al (LHCb Collaboration), Phys. Rev. D, **87**(11): 112009 (2013), arXiv:1304.6317[hep-ex]

2 R. Aaij et al (LHCb Collaboration), Phys. Rev. D, **98**(7): 072006 (2018), arXiv:1807.01891[hep-ex]

3 R. Aaij et al (LHCb Collaboration), arXiv: 1901.05745 [hep-ex].

4 R. Aaij et al (LHCb Collaboration), Phys. Rev. Lett., **112**(1): 011801 (2014), arXiv:1310.4740[hep-ex]

5 R. Aaij et al (LHCb Collaboration), Phys. Rev. Lett., **111**: 101801 (2013), arXiv:1306.1246[hep-ex]

6 T. W. Yeh and H. n. Li, Phys. Rev. D, **56**: 1615 (1997), arXiv:hep-ph/9701233

7 H. n. Li, Prog. Part. Nucl. Phys., **51**: 85 (2003), arXiv:hep-ph/0303116

8 H. n. Li and H. L. Yu, Phys. Rev. D, **53**: 2480 (1996), arXiv:hep-ph/9411308

9 A. Ali, G. Kramer, Y. Li et al, Phys. Rev. D, **76**: 074018 (2007), arXiv:hep-ph/0703162[HEP-PH]

10 S. Aoki et al (Flavour Lattice Averaging Group), arXiv: 1902.08191 [hep-lat]

11 T. Kurimoto, H. n. Li, and A. I. Sanda, Phys. Rev. D, **67**: 054028 (2003), arXiv:hep-ph/0210289

12 H. n. Li, C. D. Lu, and F. S. Yu, Phys. Rev. D, **86**: 036012 (2012), arXiv:1203.3120[hep-ph]

13 R. H. Li, C. D. Lu, W. Wang et al, Phys. Rev. D, **79**: 014013

(2009), arXiv:0811.2648[hep-ph]
14 C. S. Kim, R. H. Li, and W. Wang, Phys. Rev. D, **88**(3): 034003 (2013), arXiv:1305.5320[hep-ph]
15 W. F. Wang and Z. J. Xiao, Phys. Rev. D, **86**: 114025 (2012), arXiv:1207.0265 [hep-ph]
16 H. Y. Cheng, C. K. Chua, and K. C. Yang, Phys. Rev. D, **73**: 014017 (2006), arXiv:hepph/0508104
17 H. n. Li, Y. L. Shen, and Y. M. Wang, Phys. Rev. D, **85**: 074004 (2012), arXiv:1201.5066 [hep-ph]
18 C. D. Lü, Y. L. Shen, Y. M. Wang et al, JHEP, **1901**: 024 (2019), arXiv:1810.00819[hep-ph]
19 R. H. Li, C. D. Lu, and Y. M. Wang, Phys. Rev. D, **80**: 014005 (2009), arXiv:0905.3259[hep-ph]
20 Y. M. Wang and Y. L. Shen, Nucl. Phys. B, **898**: 563 (2015), arXiv:1506.00667[hepph]
21 H. n. Li, Y. L. Shen, Y. M. Wang et al, Phys. Rev. D, **83**: 054029 (2011), arXiv:1012.4098[hep-ph]
22 Y. Li, C. D. Lu, and Z. J. Xiao, J. Phys. G, **31**: 273 (2005), arXiv:hep-ph/0308243
23 Y. Li, C. D. Lu, Z. J. Xiao et al, Phys. Rev. D, **70**: 034009 (2004), arXiv:hepph/0404028
24 W. Wang, Phys. Rev. Lett., **110**(6): 061802 (2013), arXiv:1211.4539[hep-ph]
25 C. D. Lu and W. Wang, Phys. Rev. D, **85**: 034014 (2012), arXiv:1111.1513[hep-ph]
26 P. Colangelo, F. De Fazio, and W. Wang, Phys. Rev. D, **81**: 074001 (2010), arXiv:1002.2880[hep-ph]
27 W. Wang, Y. L. Shen, Y. Li et al, Phys. Rev. D, **74**: 114010 (2006), arXiv:hepph/0609082
28 C. D. Lu and M. Z. Yang, Eur. Phys. J. C, **28**: 515 (2003), arXiv:hep-ph/0212373
29 C. D. Lu, K. Ukai, and M. Z. Yang, Phys. Rev. D, **63**: 074009 (2001), arXiv:hep-ph/0004213
30 C. D. Lü, W. Wang, Y. Xing et al, Phys. Rev. D, **97**(11): 114016 (2018), arXiv:1802.09718[hep-ph]
31 C. H. Chen and H. n. Li, Phys. Lett. B, **561**: 258 (2003), arXiv:hep-ph/0209043
32 C. H. Chen and H. n. Li, Phys. Rev. D, **70**: 054006 (2004), arXiv:hep-ph/0404097
33 H. Y. Cheng and C. K. Chua, Phys. Rev. D, **88**: 114014 (2013), arXiv:1308.5139[hep-ph]
34 Y. Li, Sci. China Phys. Mech. Astron., **58**(3): 031001 (2015), arXiv:1401.5948 [hep-ph]
35 Y. Li, A. J. Ma, Z. Rui et al, Nucl. Phys. B, **924**: 745 (2017), arXiv:1708.02869[hep-ph]
36 H. Y. Cheng and C. K. Chua, Phys. Rev. D, **89**(7): 074025 (2014), arXiv:1401.5514 [hep-ph]
37 Y. J. Shi, W. Wang, and S. Zhao, Eur. Phys. J. C, **77**(7): 452 (2017), arXiv:1701.07571[hep-ph]
38 Y. J. Shi and W. Wang, Phys. Rev. D, **92**(7): 074038 (2015), arXiv:1507.07692 [hepph]
39 W. Wang and R. L. Zhu, Phys. Lett. B, **743**: 467 (2015), arXiv:1502.05104 [hep-ph]
40 U. G. Meißner and W. Wang, JHEP, **1401**: 107 (2014), arXiv:1311.5420 [hep-ph]
41 Z. Rui, Y. Li, and W. F. Wang, Eur. Phys. J. C, **77**(3): 199 (2017), arXiv:1701.02941[hep-ph]
42 W. F. Wang, H. n. Li, W. Wang et al, Phys. Rev. D, **91**(9): 094024 (2015), arXiv:1502.05483[hep-ph]
43 A. J. Ma, Y. Li, W. F. Wang et al, Nucl. Phys. B, **923**: 54 (2017), arXiv:1611.08786 [hep-ph]
44 A. J. Ma, Y. Li, W. F. Wang et al, Chin. Phys. C, **41**(8): 083105 (2017), arXiv:1701.01844[hep-ph]
45 Y. Li, A. J. Ma, W. F. Wang et al, Eur. Phys. J. C, **76**(12): 675 (2016), arXiv:1509.06117[hep-ph]
46 U. G. Meißner and W. Wang, Phys. Lett. B, **730**: 336 (2014), arXiv:1312.3087[hep-ph]
47 S. Cheng, Phys. Rev. D, **99**(5): 053005 (2019), arXiv:1901.06071[hep-ph]
48 R. Aaij et al (LHCb Collaboration), Phys. Rev. D, **89**(9): 092006 (2014), arXiv:1402.6248 [hep-ex]
49 S. M. Flatte, Phys. Lett. B, **63**: 228 (1976)
50 Y. Y. Keum, T. Kurimoto, H. N. Li et al, Phys. Rev. D, **69**: 094018 (2004), arXiv:hep-ph/0305335
51 D. Müller, D. Robaschik, B. Geyer et al, Fortsch. Phys., **42**: 101 (1994), arXiv:hep-ph/9812448
52 M. Diehl, T. Gousset, B. Pire et al, Phys. Rev. Lett., **81**: 1782 (1998), arXiv:hepph/9805380
53 M. V. Polyakov, Nucl. Phys. B, **555**: 231 (1999), arXiv:hep-ph/9809483
54 M. Alston-Garnjost, A. Barbaro-Galtieri, S. M. Flatte et al, Phys. Lett. B, **36**: 152 (1971)
55 S. M. Flatte, M. Alston-Garnjost, A. Barbaro-Galtieri et al, Phys. Lett. B, **38**: 232 (1972)
56 S. M. Flatte, Phys. Lett. B, **63**: 224 (1976)
57 G. Buchalla, A. J. Buras, and M. E. Lautenbacher, Rev. Mod. Phys., **68**: 1125 (1996), arXiv:hep-ph/9512380
58 J. Beringer et al (Particle Data Group), Phys. Rev. D, **86**: 010001 (2012)
59 K. A. Olive et al (Particle Data Group), Chin. Phys. C, **38**: 090001 (2014)
60 R. Aaij et al (LHCb Collaboration), Phys. Rev. D, **90**(1): 012003 (2014), arXiv:1404.5673 [hep-ex]
61 R. Aaij et al (LHCb Collaboration), JHEP, **1508**: 005 (2015), arXiv:1505.01654[hep-ex]
62 W. Wang, Phys. Rev. D, **85**: 051301 (2012), arXiv:1110.5194 [hep-ph]
63 M. Tanabashi et al (Particle Data Group), Phys. Rev. D, **98**(3): 030001 (0300)
64 W. Wang, Int. J. Mod. Phys. A, **29**: 1430040 (2014), arXiv:1407.6868[hep-ph]
65 A. Cerri et al, arXiv: 1812.07638 [hep-ph]